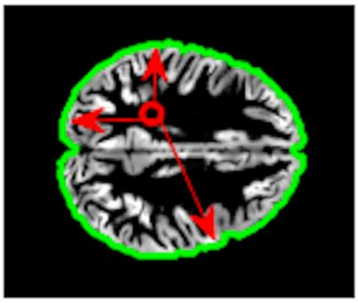

Figure S1: Spatial series extraction. The green line corresponds to the outer boundary and the red dot depicts the center of mass of the whole GM brain.

Largest Lyapunov Exponent

One of the best-known methods for quantitative assessment of chaos is the Largest-Lyapunov-Exponent (lambda). A positive lambda expresses sensitive dependence on initial conditions for a dynamical system. A positive lambda presents the average rate over the whole attractor, at which two nearby trajectories become exponentially separate with time evolution (Alexandra I. Korda, Asvestas, Matsopoulos, Ventouras, & Smyrnis, 2018). A practical numerical technique for calculating lambda is the method developed by Rosenstein et al. (Rosenstein, Collins, & De Luca, 1993), which works well with small datasets and is robust to changes in the embedding dimension, reconstruction delay, and noise level (Takens, 1981). In brief, let x_i denote the spatial series of the distances extracted from the brain sMRI. If it is assumed that the given spatial-series provides an observation of a dynamical system, then according to the theorem of Takens (Takens, 1981), the trajectory of the attractor of the system can be described by a matrix X. Takens Theorem is not restricted to time series. It is necessary that the series is determined by a trajectory in a finite state-space. Even if this is not exactly given, one can apply the procedure of determining lambda and regard lambda as a feature describing structural aspects of the cortex. Each row, X_k, of the matrix is a state space vector:

$$X_k = \left[x_k, x_{k+\tau}, x_{k+2\tau}, \dots, x_{k+(m-1)\tau}\right] \quad (1)$$

where $k = 0,1,\dots,M-1$, $M = N-(m-1)\tau$, N is length of the spatial-series, τ and m are the embedding delay and the embedding dimension, respectively (Kennel et al., 1992; Strogatz, 2015).

After the state space reconstruction, the lambda can be defined using the following equation:

$$d(t) = d(0)e^{\lambda_1 t} \quad (2)$$

where λ_1 is the lambda value, $d(t)$ is the average divergence at the voxel t, and $d(0)$ is a constant that normalizes the initial separation.

Lambda can be estimated using the matrix X of the reconstructed state space as in (Alexandra I. Korda et al., 2018). A spatial-dependent value of lambda, $\lambda_1(k)$, where k is the target voxel and T the distance between voxels in the state space, can be estimated as:

$$\lambda_1(k) = \frac{\langle lnd(k)\rangle - \langle lnd(k-1)\rangle}{T}, k > 1 \quad (3)$$

Third party code used for the calculation of the Lambda and it is available online (https://www.mathworks.com/matlabcentral/fileexchange/38424-largest-lyapunov-exponent-with-rosenstein-s-algorithm), MATLAB Central File Exchange.

Wavelet Transformation

The wavelet transform (WT) employs a fully scalable modulated window, which provides an extensively tested solution to the windowing function selection problem in frequency-related (scale-related) signal processing methodologies. The window is sliding across the signal, and for every position a spectrum is calculated. The procedure is then repeated at a multitude of scales, providing a signal representation with multiple spatial-scale resolutions. It does not only inform us on which scales are present in a signal, but also at which geometrical point these scales are presented. This allows for good point resolution for high-scale events, as well as good scale resolution for low-scale events, which is a combination of properties particularly well-suited to real signals. The rationale of the WT approach is that, firstly, the signal is "viewed" at a large scale/window and "large" features are analyzed and then the signal is "viewed" at smaller scales, in order to analyze "smaller" features (A. I. Korda et al., 2022). In the present work continuous wavelet transform (CWT) was used for extracting features from lambda series obtained from the three types of groups that were described above. CWT was used to decompose the lambda series into their frequency components and the statistical features of the CWT coefficients were computed in the spatial domain. A CWT with a complex Morlet as mother function was used, see **Figure S2.**

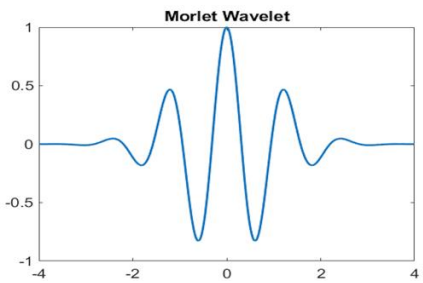

Figure S2. Morlet wavelet

The WT of a 1-dimensional (1D) series has two dimensions. This 2-dimensional (2D) output of the WT provides the spatial-scale representation of the original series in the form of a "scalogram" plane. The two dimensions of a scalogram are the geometrical points and the scales. Each value (wavelet coefficient) in the scalogram plane represents the correlation of the lambda series with the Morlet wavelet on the respective point and scale pair.

Table 1 Group comparison was investigated using 1-way ANOVA for continuous and χ^2 test for categorical data.

One-Way ANOVA (Welch's)		
FEP vs HC	**F**	**p**
Age	1.63	0.204
Education (Years)	19.26	< .001
Smoking (Cigarettes per Day)	28.18	< .001
CHR vs HC		
Age	2.082	0.152
Education (Years)	10.654	0.002
Smoking (Cigarettes per Day)	8.634	0.004
FEP vs. CHR		
Age	3.118	0.056
Education (Years)	0.165	0.849
Global Assessment of Functioning (GAF)	46.875	< .001
BPRS_Positive_Symptoms	19.498	< .001
BPRS_Negative_Symptoms	22.494	< .001
BPRS_total	462.930	< .001
SANS_total	128.957	< .001
Smoking (Cigarettes per Day)	2.418	0.102
χ^2 Tests		
FEP vs. HC		
Sex	13.6	< .001
Alcohol	9.60	0.008
CHR vs. HC		
Sex	17.7	< .001
Alcohol	0.14	0.710
FEP vs. CHR		
Sex	0.431	0.511
Alcohol	2.80	0.246

Note: BPRS, Brief Psychiatric Rating Scale; GAF, Global Assessment of Functioning; SANS, Scale for the Assessment of Negative Symptoms

Below in **Figure S3**, the scalograms of FEP are labelled with [1] and the scalograms of HC are labeled with [0].

Appendix 1 to: Korda AI, Andreou C, Avram M, et al. Chaos analysis of the cortical boundary for the recognition of psychosis. *J Psychiatry Neurosci* 2023. doi: 10.1503/jpn.220160.

Appendix 1 to: Korda AI, Andreou C, Avram M, et al. Chaos analysis of the cortical boundary for the recognition of psychosis. *J Psychiatry Neurosci* 2023. doi: 10.1503/jpn.220160.

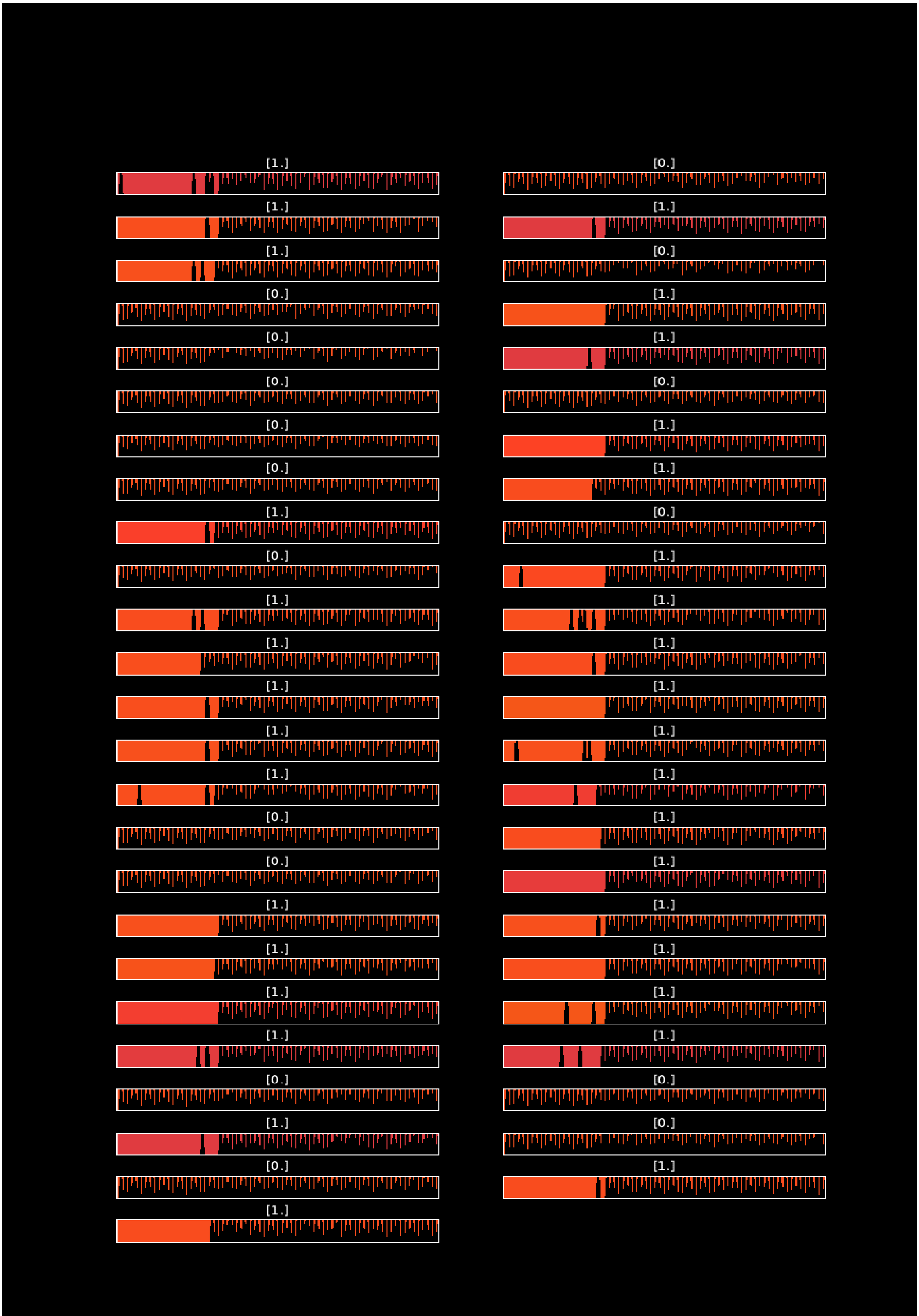

Appendix 1 to: Korda AI, Andreou C, Avram M, et al. Chaos analysis of the cortical boundary for the recognition of psychosis. *J Psychiatry Neurosci* 2023. doi: 10.1503/jpn.220160.

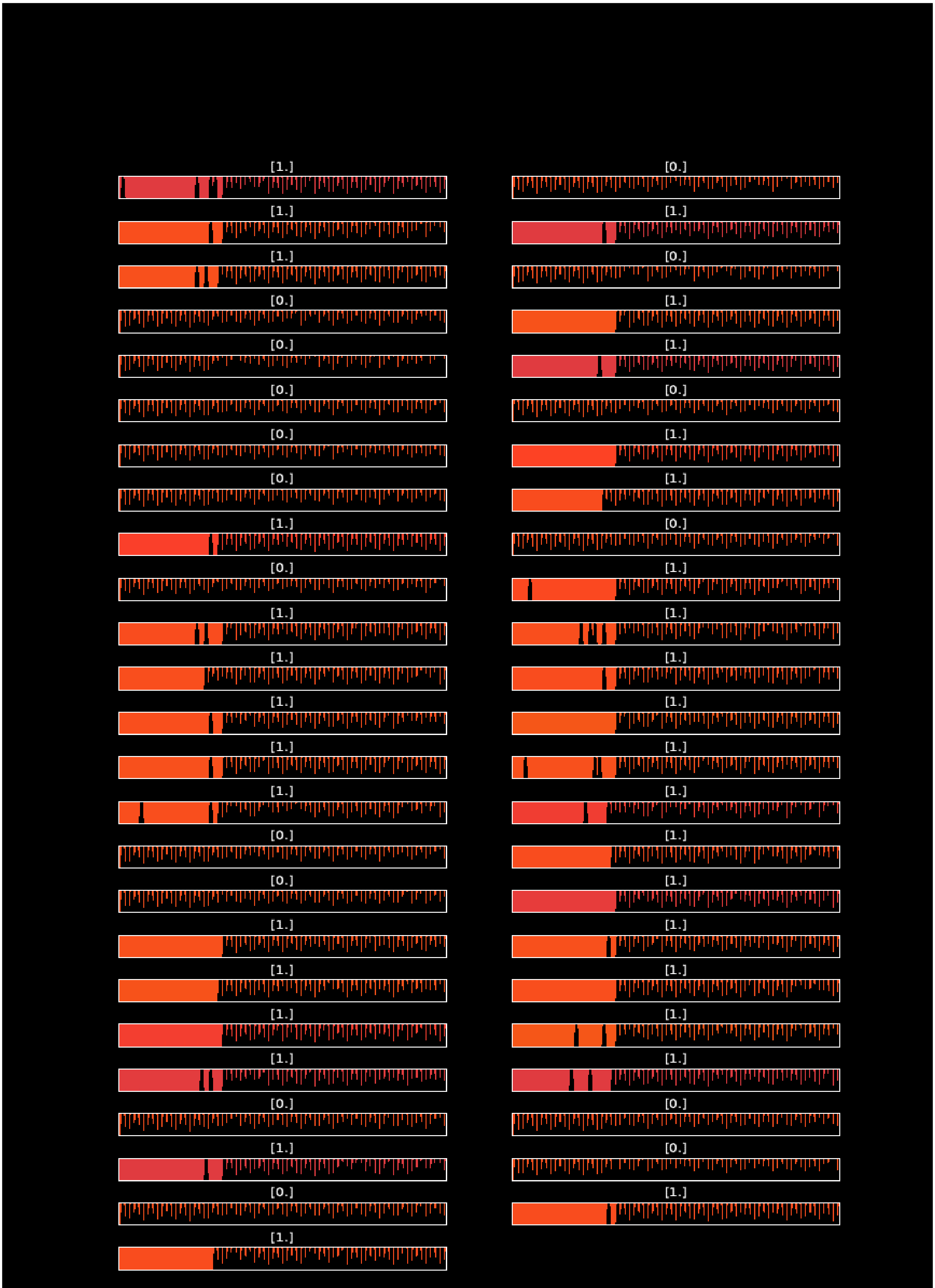

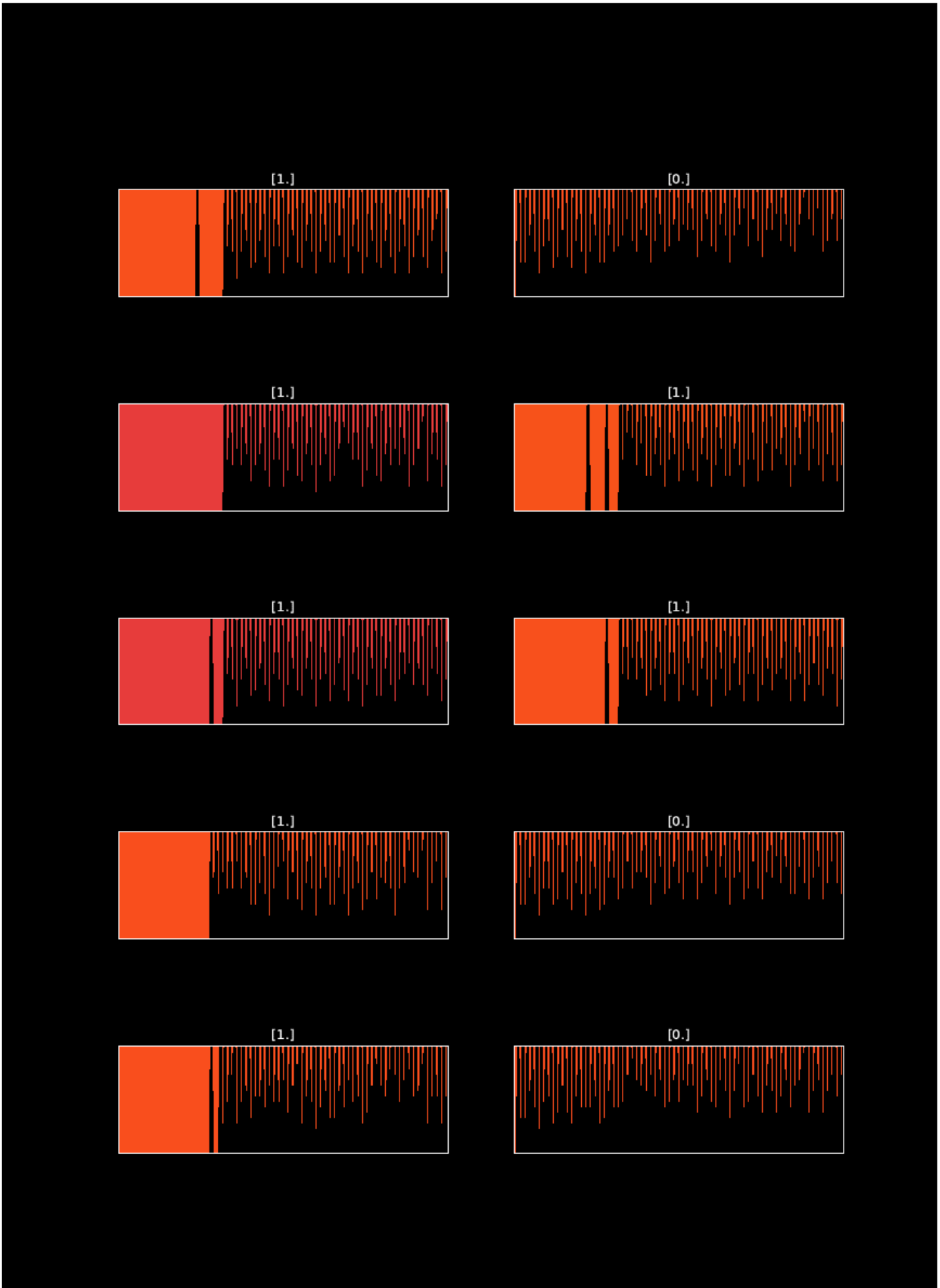

Appendix 1 to: Korda AI, Andreou C, Avram M, et al. Chaos analysis of the cortical boundary for the recognition of psychosis. *J Psychiatry Neurosci* 2023. doi: 10.1503/jpn.220160.

Below in **Figure S4,** the scalograms of FEP are labelled with [1] and the scalograms of CHR are labeled with [0].

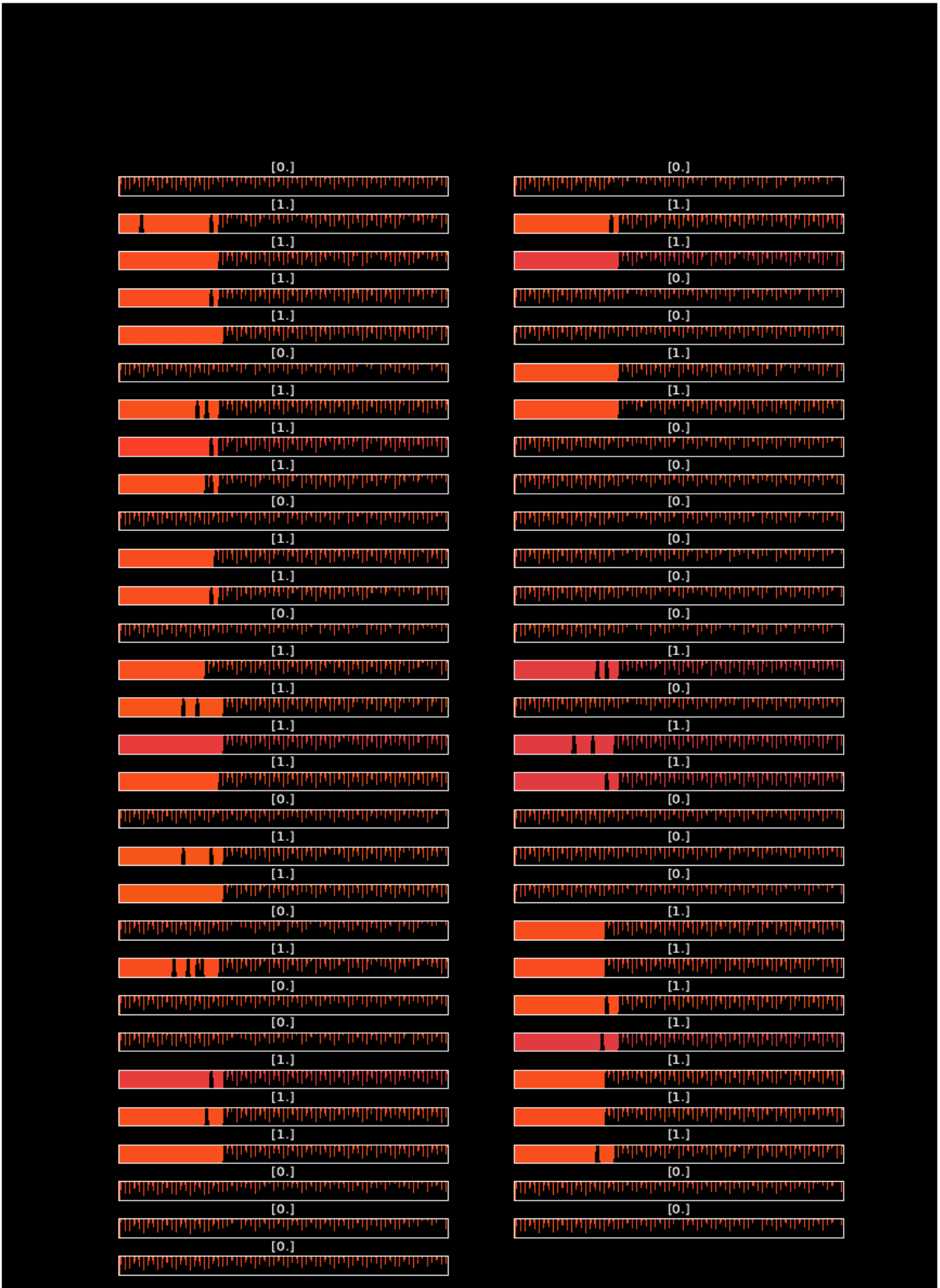

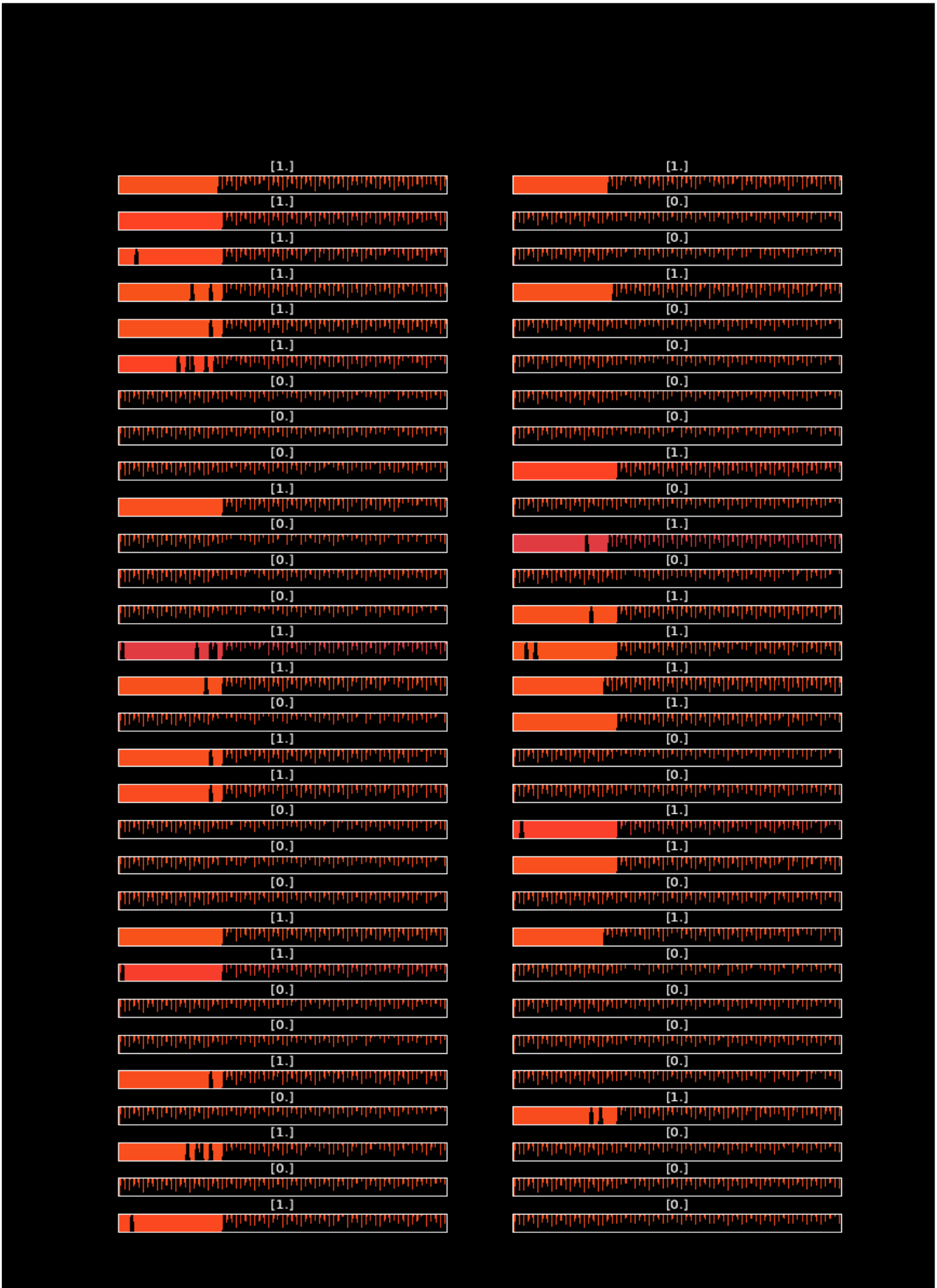

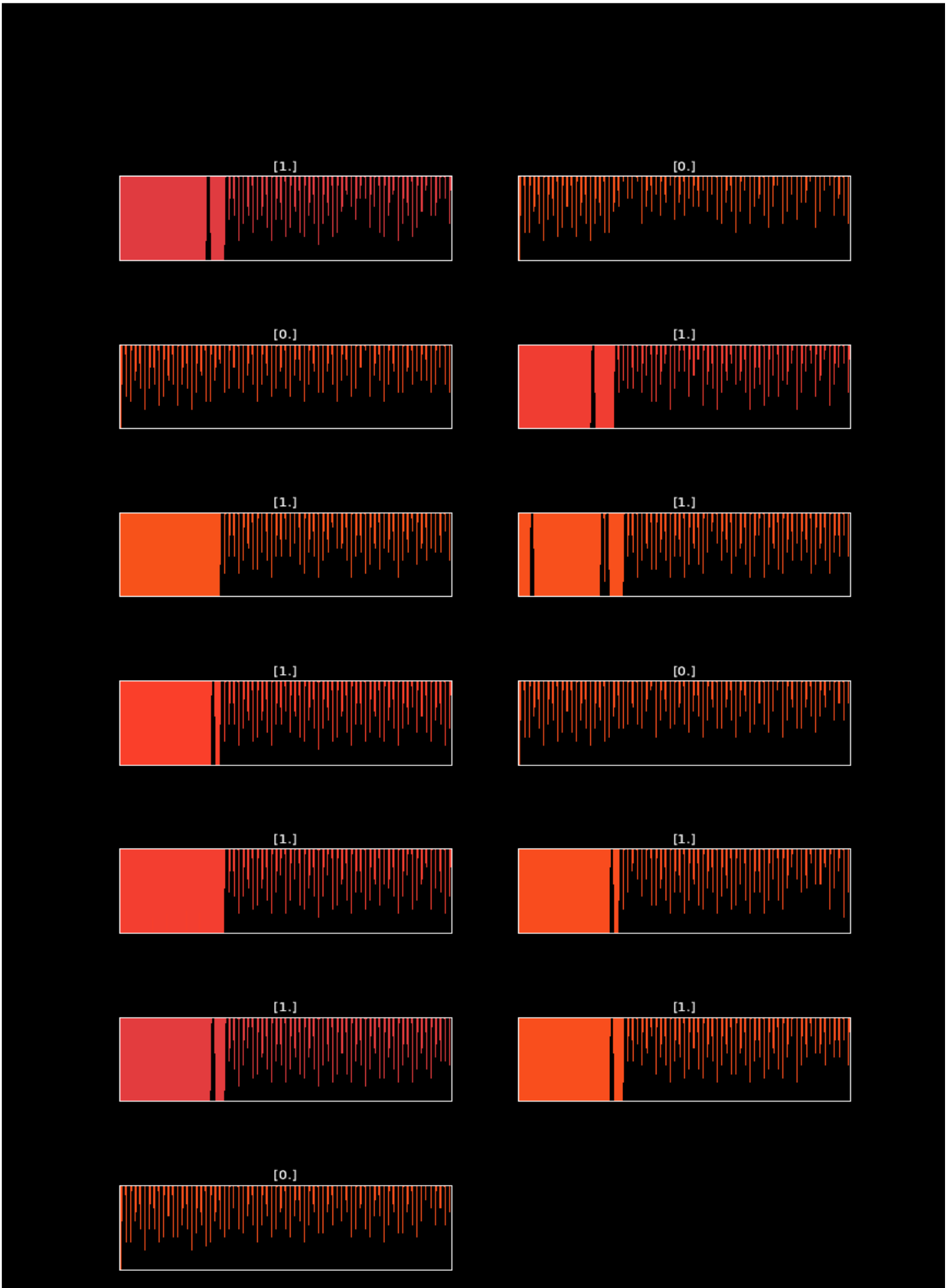

Appendix 1 to: Korda AI, Andreou C, Avram M, et al. Chaos analysis of the cortical boundary for the recognition of psychosis. *J Psychiatry Neurosci* 2023. doi: 10.1503/jpn.220160.

Kennel, M. B., Brown, R., & Abarbanel, H. D. I. (1992). Determining embedding dimension for phase-space reconstruction using a geometrical construction. *Physical Review A, 45*(6), 3403-3411. doi:10.1103/PhysRevA.45.3403

Korda, A. I., Asvestas, P. A., Matsopoulos, G. K., Ventouras, E. M., & Smyrnis, N. (2018). Automatic identification of eye movements using the largest lyapunov exponent. *Biomedical Signal Processing and Control, 41*, 10-20. doi:https://doi.org/10.1016/j.bspc.2017.11.004

Korda, A. I., Ventouras, E., Asvestas, P., Toumaian, M., Matsopoulos, G. K., & Smyrnis, N. (2022). Convolutional neural network propagation on electroencephalographic scalograms for detection of schizophrenia. *Clinical Neurophysiology, 139*, 90-105. doi:https://doi.org/10.1016/j.clinph.2022.04.010

Rosenstein, M. T., Collins, J. J., & De Luca, C. J. (1993). A practical method for calculating largest Lyapunov exponents from small data sets. *Physica D: Nonlinear Phenomena, 65*(1), 117-134. doi:https://doi.org/10.1016/0167-2789(93)90009-P

Strogatz, S. H. (2015). *Nonlinear Dynamics and Chaos: With Applications to Physics, Biology, Chemistry, and Engineering (2nd ed.).* .

Takens, F. (1981, 1981//). *Detecting strange attractors in turbulence.* Paper presented at the Dynamical Systems and Turbulence, Warwick 1980, Berlin, Heidelberg.